IIETA International Information and Engineering Technology Association
Advancing the World of Information and Engineering

Journal Européen des Systèmes Automatisés
Vol. 57, No. 6, December, 2024, pp. 1705-1711
Journal homepage: http://iieta.org/journals/jesa

Position and Speed Control for Permanent Magnet DC Motor Based on Different Optimization Algorithms

Diyah Kammel Shary[1], Habeeb J. Nekad[2*]

[1] Department of Electrical Engineering Techniques, Southern Technical University, Basrah 61001, Iraq
[2] Department of Electrical Engineering, University of Basrah, Basrah 61001, Iraq

Corresponding Author Email: habeeb.nekad@uobasrah.edu.iq

https://doi.org/10.18280/jesa.570618

Received: 11 November 2024
Revised: 27 November 2024
Accepted: 6 December 2024
Available online: 31 December 2024

Keywords:
Ant Colony Optimization, Flower Pollination Algorithm, Grey Wolf Optimization, PID controller, PMDC motor

ABSTRACT

This paper focused on the position and speed control of Permanent Magnet DC (PMDC) motor based on Proportional-Integral-Derivative (PID) controller. The mathematical model of PMDC motor is presented with aid of Matlab /Simulink which shows the main equations of these motors. The optimum values of PID parameters are evaluated according to three different optimization algorithms: Ant Colony Optimization (ACO) which is based on cooperative behavior of real ant colonies, Grey Wolf Optimization (GWO) is a nature-inspired meta-heuristic algorithm inspired by the social hierarchy and hunting behavior of grey wolves, and Flower Pollination Algorithm (FPA) is an algorithm inspired by the process of flower pollination. Position and speed of PMDC motor are investigated under different conditions of operation. According to the simulation results, employing optimization techniques improves the performance of conventional PID controllers to provide a better response for the motor. Finally, the results of the comparison in terms of speed and position of the motor show that the use of algorithms in the PID controller will improve the behavior (overshoot and settling time) of the motor significantly compared with the conventional PID controller at different loading conditions. The oscillations will be reduced effectively and clearly with optimum values of error.

1. INTRODUCTION

Permanent Magnet DC motors (PMDC), that are typical, fundamental forms of DC motors, are frequently utilized, despite the widespread usage of Brushless DC motors (BLDC) in numerous fields. PMDC motor is one of the prime movers that is currently employed the most in industry. There are numerous applications for PMDC motors, including electric tracking systems, robotic manipulators, electric vehicles, and textile mills including weaving and spinning [1-4].

PMDC motor performance can be improved by adjusting position and/or speed control. Due to their ease of use and reliable performance, a lot of systems employ proportional integral derivative (PID) controllers. Thus, modifying the PID parameters has long been a prominent research area [5, 6]. Furthermore, PID controller constants can be modified using optimization or computational methods.

For PMDC motors, different techniques have recently been widely suggested. Researchers presented a comparison of the PID controller tuned using two distinct methods in 2011: Particle Swarm Optimization (PSO) and Genetic Algorithm (GA). The work of both controllers gave a description of the main characteristics of each one [7].

The study [8] created a PID controller (self-tuning) in 2013 to manage the speed of PMDC motors. The variables were adjusted to satisfy the specifications that were examined using the experimental results. The study [9] were given the following comparison of various approaches: cascade PI(D) controller parameters are adjusted using the Classical Method (CM), Bacterial Foraging Algorithm (BFA), and Genetic Algorithm (GA). The PMDC motor's speed was controlled, and its performance and stability were enhanced using PI and Fuzzy Logic (FL) controllers [10].

PI and PID controllers in single and cascade configurations were developed to construct a dependable controller with high disturbance rejection [11]. Standard PSO, dynamic PSO with constant and variable inertia weight algorithms, Artificial Bee Colonies (ABC), and Ant Colony Optimization (ACO) algorithms were all the subject of research in 2017. These methods can be used to estimate a PMDC motor variables in conjunction with experimental tests [12].

To manage the speed of the PMDC while taking into account the non-linear behavior of armature resistance, a fractional order PID (FOPID) controller is proposed in place of an integer-order PID controller. Both the two controllers are simulated, and their responses are examined under various operating situations [13].

In 2021, the PID gains for the cascade controller of a PMDC motor were extracted using two optimization techniques: PSO and Butterfly Optimization Algorithm (BOA) [14]. The efficacy of improving a controller architecture for a PMDC motor will be examined in 2022. The PID controller controls the PMDC motor speed using two distinct neural network-based methods [15]. In 2024, researchers [16] introduced a

nonlinear PI controller for improved speed regulation in PMDC motor drive systems.

In this paper, PID controllers of PMDC motor speed and position are tuned with aid of (Ant Colony Optimization (ACO), Grey Wolf Optimization (GWO), and Flower Pollination Algorithm (FPA)). PMDC motor is tested under different conditions of operation. Where the addition of these algorithms in PID controllers give effectiveness method to improve the motor performance under different work conditions.

2. METHODOLOGY

2.1 Dynamic model of PMDC motor

Figure 1 displays a schematic diagram of PMDC motor. This motor differs from conventional DC motors in that it without field circuit, and instead the permanent magnet is used to produce a field flux.

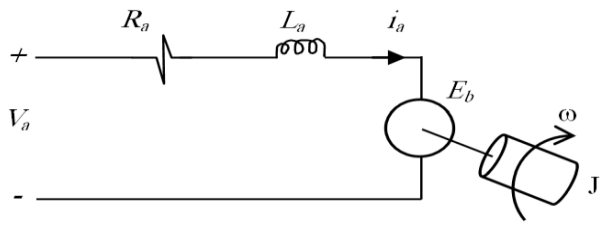

Figure 1. Schematic diagram of PMDC motor

The following equations give the dynamic model of the PMDC motor [7, 8, 12, 17, 18]:

$$V_a(t) = R_a i_a(t) + L_a \frac{di_a(t)}{dt} + E_b \tag{1}$$

$$E_b = k_v \omega(t) \tag{2}$$

$$T_e = J\frac{d\omega(t)}{dt} + B\omega(t) + T_L \tag{3}$$

$$T_e = k_t i_a(t) \tag{4}$$

$$\omega(t) = \frac{d\theta(t)}{dt} \tag{5}$$

where, V_a and i_a, respectively, are the armature voltage and current, E_b is the back e.m.f., T_e is the electromagnetic torque, T_L is the load torque, ω is the motor angular speed, θ is the motor angular position, J is the rotor's inertia and the equivalent mechanical load, B is the motor's mechanical rotational system's damping coefficient, k_v stands for velocity constant, and k_t is the torque constant.

The following differential equations can be formed by rearranging Eqs. (1)-(4):

$$\frac{\mathrm{di_a(t)}}{\mathrm{dt}} = \frac{\mathrm{V_a(t)}}{\mathrm{L_a}} - \frac{\mathrm{R_a}}{\mathrm{L_a}}\mathrm{i_a(t)} - \frac{\mathrm{k_v}}{\mathrm{L_a}}\omega(\mathrm{t}) \tag{6}$$

$$\frac{\mathrm{d\omega(t)}}{\mathrm{dt}} = \frac{\mathrm{k_t}}{\mathrm{J}}\mathrm{i_a(t)} - \frac{\mathrm{B}}{\mathrm{J}}\omega(\mathrm{t}) - \frac{1}{\mathrm{J}}\mathrm{T_L} \tag{7}$$

By taking Laplace transform of (6) and (7), the armature current and angular speed equations are expressed as:

$$I_a(s) = \frac{1}{(L_a s + R_a)}[V_a(s) - k_v \Omega(s)] \tag{8}$$

$$\Omega(s) = \frac{1}{(Js + B)}[k_t I_a(s) - T_L(s)] \tag{9}$$

Also, equation of the angular position in Laplace transform is written as:

$$\Theta(s) = \frac{\Omega(s)}{s} \tag{10}$$

According to the above equations, Figure 2 displays the PMDC motor's block diagram.

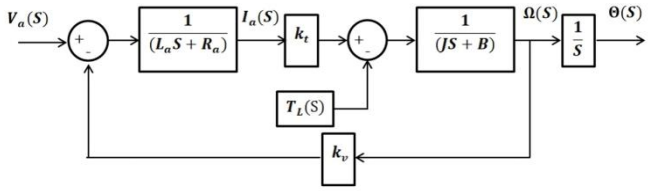

Figure 2. PMDC motor block diagram

2.2 PID controller

A conventional PID can be considered as a foundation stone algorithm in the theory of control. Many systems use this control algorithm because it is smooth and precise. Different constant parameters employed in the PID controller approach include proportional, integral, and derivative values. Trial and error are one of the methods for adjusting these values. The control decision of the regulation is set mathematically according to [8, 19, 20]:

$$u(t) = K_P e(t) + K_I \int e(t)dt + K_D \frac{de(t)}{dt} \tag{11}$$

where, K_P is the proportional constant, K_I represents the integral constant, K_D indicates the derivative constant, $u(t)$ is the output waveform, and $e(t)$ is the error waveform.

2.3 Ant Colony Optimization (ACO)

ACO algorithm is a meta-heuristic computer optimization methodology that utilizes the nature-derived optimization approach. Marco Dorigo has proposed ACO method which was developed with the use of ants as inspiration in order to find the best route between food and the nest. When ants are looking for food, they first randomly investigate the area around their colony. The ants move across the ground and leave a chemical pheromone trail. For pheromone quantity, two main conditions must be satisfied: a path length and discovered food source quality [12, 21-24].

ACO algorithm can be summarized as:

1) Initialization: All ACO algorithm parameters are initialized such as n: nodes number, m: ants number, t_{max}: maximum iteration, d_{max}: maximum distance for each ant's tour, α: pheromone decay parameter ($0<\alpha<1$), β: relative importance of pheromone versus distance ($\beta>1$), ρ : heuristically defined coefficient ($0<\rho<1$), q_a : algorithm

parameter, and τ_0: a level of initial pheromone.

A maximum distance for each ant's tour d_{max} is given as [25]:

$$d_{max} = max\left[\sum_{i=1}^{n-1} d_i\right] \quad (12)$$

$$d_i = |r - max\ (u)| \quad (13)$$

where, d_i is the separate distance between two nodes, r is the current node, and u is the unvisited node.

2) Generate first position randomly according to uniform distribution.

3) The probability of an ant (k) at node (i) selecting the next node (j) is given by:

$$p_{ij}^k(t) = \frac{[\tau_{ij}(t)]^\alpha [\eta_{ij}(t)]^\beta}{\sum_{ij\epsilon T^k}[\tau_{ij}(t)]^\alpha [\eta_{ij}(t)]^\beta}; \qquad ij\epsilon T^k \quad (14)$$

where, τ_{ij} is the trial of pheromone deposited by ant k between node i and j, ($\eta_{ij} = 1/d_{ij}$) is the visibility, and T^k is the route implemented by the ant k at a known time.

4) Local pheromone updating: which is not similar for all ants since every ant follows a different path. Each ant's original pheromone is locally updated as:

$$\tau_{ij}(t+1) = (1-\rho)\tau_{ij}(t) + \rho\tau_0 \quad (15)$$

5) When the strongest pheromone draws ants along the shortest path, the aim function is most effectively carried out.

6) The following formulae can be used to update global pheromone:

$$\tau_{ij}(t+1) = (1-\alpha)\tau_{ij}(t) + \alpha\Delta\tau_{ij}(t) \quad (16)$$

7) The best outcome is attained when every ant takes the same best course. If not, the procedure goes on until the iteration's conclusion.

2.4 Grey Wolf Optimization (GWO)

The GWO technique, a meta-heuristic algorithm, was introduced [26-28] and mimics grey wolves' social behavior. Between 5 and 12 wolves make up the group that lives together. This group follows the rigid dominance hierarchy, with a leader α and supporting member β who assist the leader in making decisions. δ and ω are the rest members of the group as shown in Figure 3.

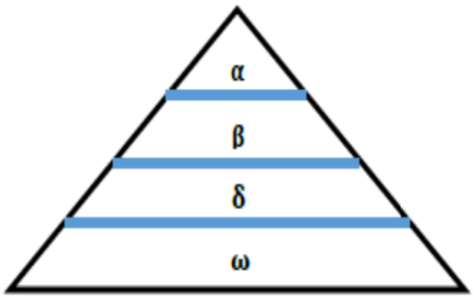

Figure 3. Social hierarchy of GWO

Additionally, the primary activity for all of the wolves is hunting for prey by searching for it and attacking it. Firstly, the wolves will surround their victim before attacking it. The equations below show the mathematical model of the prey being encircled [28-30]:

$$\vec{D} = \left|\vec{C}.\vec{X}_p(t) - \vec{X}(t)\right| \quad (17)$$

$$\vec{X}(t+1) = \vec{X}_p(t) - \vec{A}.\vec{D} \quad (18)$$

where, $\vec{D}$ is the distance vector, $\vec{X}_p(t)$ stands the vector of the prey's position, $\vec{X}(t)$ is the wolf position vector, and t is the current iteration. $\vec{A}$, $\vec{C}$ are coefficient vectors which can be determined as:

$$\vec{A} = 2\vec{a}.\vec{r}_1 - \vec{a} \quad (19)$$

$$\vec{C} = 2.\vec{r}_2 \quad (20)$$

where, $\vec{r}_1$ and $\vec{r}_2$ are the random vectors in the range [0,1]. As the number of iterations rises, the value of the constant $\vec{a}$ decreases linearly from 2 to 0.

In relation to location of its prey, the position of a grey wolf shifts. In this method, with the assistance of the three currently best-known solutions (α, β, δ), the optimal solution (prey) is discovered. The following equations are used in order to update their positions in the following iteration [28-30]:

$$\left.\begin{aligned}\vec{D}_\alpha &= \left|\vec{C}_1.\vec{X}_\alpha - \vec{X}\right| \\ \vec{D}_\beta &= \left|\vec{C}_2.\vec{X}_\beta - \vec{X}\right| \\ \vec{D}_\delta &= \left|\vec{C}_3.\vec{X}_\delta - \vec{X}\right|\end{aligned}\right\} \quad (21)$$

$$\left.\begin{aligned}\vec{X}_1 &= \vec{X}_\alpha - \vec{A}_1.\vec{D}_\alpha \\ \vec{X}_2 &= \vec{X}_\beta - \vec{A}_2.\vec{D}_\beta \\ \vec{X}_3 &= \vec{X}_\delta - \vec{A}_3.\vec{D}_\delta\end{aligned}\right\} \quad (22)$$

$$\vec{X}(t+1) = \frac{\vec{X}_1 + \vec{X}_2 + \vec{X}_3}{3} \quad (23)$$

In search of a more favorable target, other wolves will depart from the current prey when the value of $\vec{A}$ is greater than 1 or less than -1, which enables the GWO algorithm's capacity to search globally. Furthermore, $\vec{C}$ values are scattered at a random distributed between 0 and 2, allowing for easier exploration during the entire method [29, 30].

2.5 Flower Pollination Algorithm (FPA)

It is thought that 80% of plants rely on flower pollination to carry pollen from a male flower to a female bloom in order to reproduce. Two types of pollination: biotic and abiotic. Only 10% of pollination is carried out by wind and other natural forces, the other 90% taking place through insects and other animals. In biotic systems, pollination occurs either through self-pollination within a single flower or through cross-pollination between two distinct flowers. Biotic and cross pollination occurs between flowers that are farther apart, which is an example of global optimization [31, 32].

The idea of FPA can be described according to the following main principles [31, 32]:

1) Global pollination is biotic and cross-pollination.

2) Local pollination is abiotic and self-pollination.

3) Stability of the flower increases the likelihood of reproduction which may be developed in the way of pollinators such as birds, insects. It largely relies on how similar the two flowers used in the reproduction process are to one another.

4) By altering probability values in the (0–1) range with a small preference for local pollination, it is possible to manage the transition between local and global pollination.

In FPA algorithm, the answer X_i is comparable to a flower and/or a pollen gamete. Pollinators transport flower pollens for global pollination. With Lévy flight, pollens are capable of traveling far. Therefore, the main principles 1 and 3 can be expressed as [31-34]:

$$X_i^{t+1} = X_i^t + L(X_i^t - g^*) \tag{24}$$

where, X_i^t stands the solution vector X_i at tth iteration, g^* represents the current best solution in the iteration among the current options, and L is the pollination strength, which is essentially a step size.

Levy flight distribution is used to simulate how insects fly over large distances while taking into consideration the fact that they move with different distance steps. Utilizing the Levy distribution, $L > 0$ can be represented as [31-34]:

$$L \approx \frac{\lambda \Gamma(\lambda) \sin\left(\frac{\pi\lambda}{2}\right)}{\pi} \frac{1}{s^{1+\lambda}}, \quad (s \gg s_0 > 0) \tag{25}$$

where, $\Gamma(\lambda)$ is the standard gamma function, and for big steps $s > 0$, this distribution is valid.

For local pollination, main principles 2 and 3 are represented by the following [31-34]:

$$X_i^{t+1} = X_i^t + \epsilon(X_i^t - X_k^t) \tag{26}$$

where, X_i and X_k are pollen grains from various blooms of the same type of plant, while ε represents a random walk in which the distribution is uniformed between 0 and 1.

At the end, new solutions for all flowers are finding. If the new solutions are best, they are replaced in the population and the process is then repeated for every member of the population to identify the best current solution.

3. RESULTS AND DESCUSSION

Figure 4 displays the block diagram for the proposed PID controller-based PMDC motor control that is tuned using optimization techniques where the optimization algorithms will compute the optimum values of PID controllers.

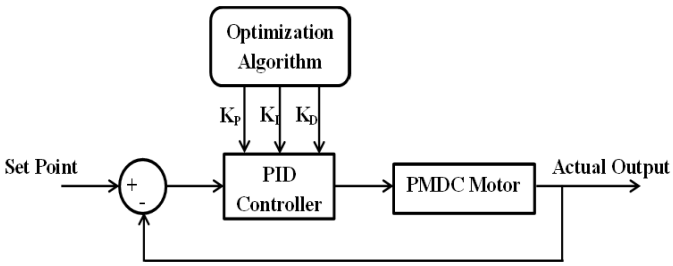

Figure 4. Block diagram of proposed control

Table 1 contains a list of PMDC motor specifications, while Table 2 and Table 3 contain the values of optimized PID controllers' constants. Also, the error values for different optimization algorithms are illustrated in these tables. Figure 5 shows the final Simulink diagram for the proposed system where the error signal is considered as the input to the control unit (Matlab version 2022a is used with automatic solver selection and variable-step).

Table 1. Specifications of PMDC motor [11]

Motor Parameters	Value
Armature Resistance	0.5 Ω
Armature Inductance	0.01 H
Inertia	0.037 Kg.m^2
Damping Coefficient	0.01 Ns/rad./sec.
Speed Constant	1.22
Torque Constant	1.22

Table 2. Controller parameters for speed

Optimization Algorithm	K_p	K_i	K_D	Error (ITAE)
ACO	0.14	15	0.02	9.8209×10^{-5}
GWO	0.01	8.367	0.01	8.1073×10^{-5}
FPA	0.4524	24.2746	0.036	8.3482×10^{-5}

Table 3. Controller parameters for position

Optimization Algorithm	K_p	K_i	K_D	Error (ITAE)
ACO	19	54.53	0.85	9.8423×10^{-5}
GWO	18	51	0.5	1.8288×10^{-5}
FPA	20.134	60	0.01	8.8253×10^{-5}

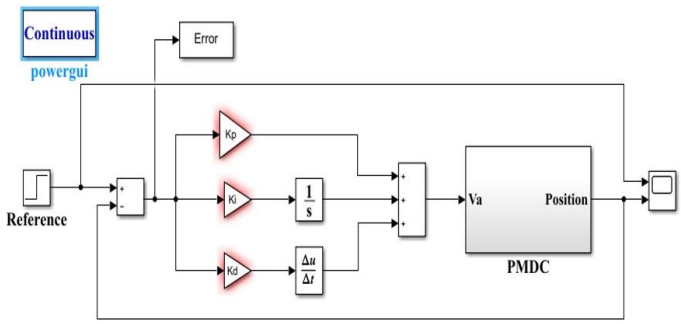

Figure 5. Simulink diagram of proposed system

Figures 6-9 illustrate the position and speed responses for the motor at different kinds of optimization algorithms under no load and load conditions. From these figures, the motor has the capability to the fast response with the changing in reference speed or position at t=1 second and to the sudden change in loading at t=5 second. After applying the PID controller's optimal values in accordance with the three different optimization algorithms, the motor's performance is enhanced.

To show the best operation of PMDC motor after applying the different optimization algorithm, armature current response is illustrated in Figures 10-12. It is clear that GWO gives the best performance as compared with ACO and FPA. Where the error value is minimum in the case of GWO as in Tables 2 and 3. The optimized parameters provide good performance in the presence of noise and disturbances as shown in Figures 6-9. Also, it can be used these algorithms in

practical cases by programming the control circuit of PMDC motor.

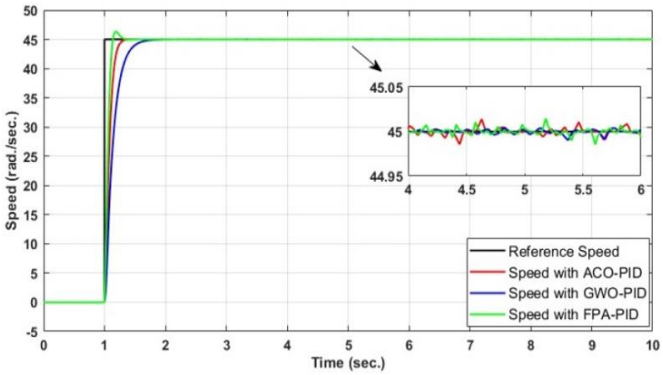

Figure 6. Motor speed at no load

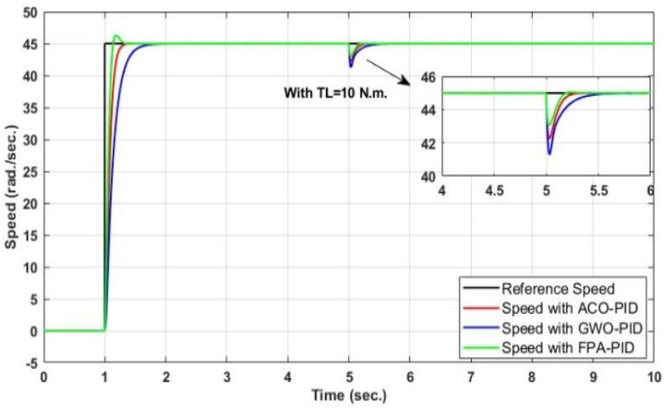

Figure 7. Motor speed with load

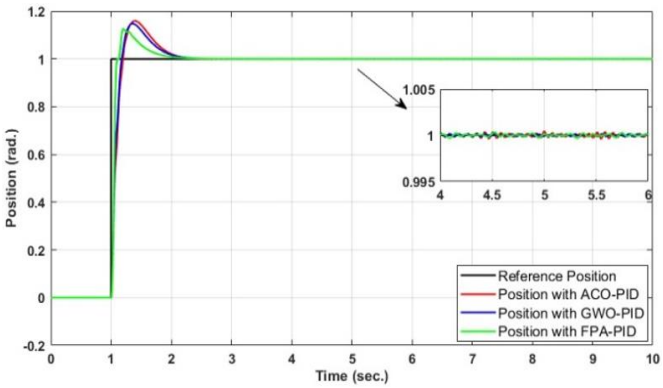

Figure 8. Motor position at no load

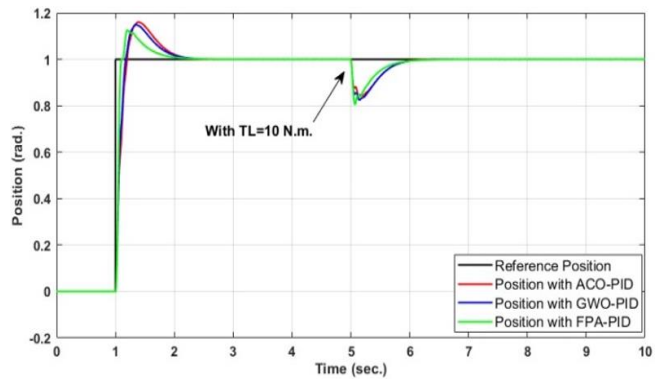

Figure 9. Motor position with load

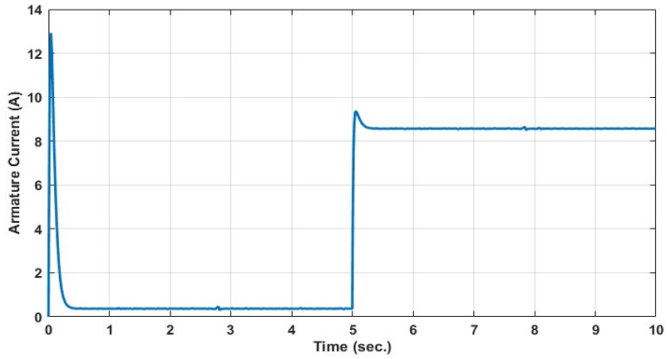

Figure 10. Armature current for PID with ACO

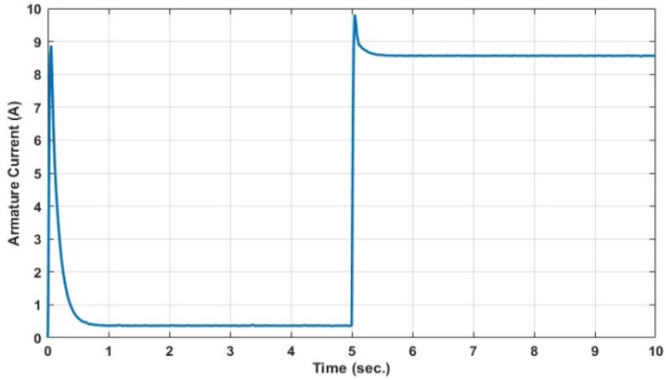

Figure 11. Armature current for PID with GWO

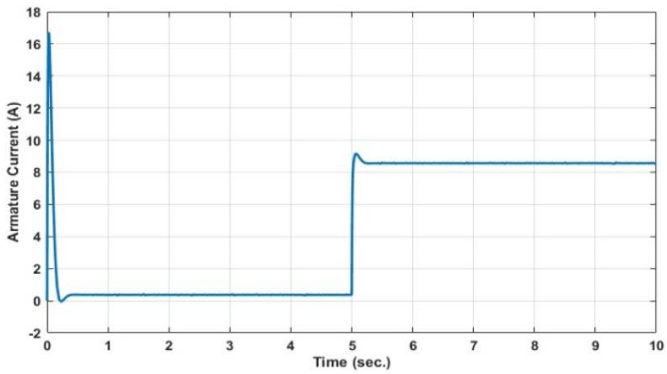

Figure 12. Armature current for PID with FPA

4. CONCLUSIONS

This paper illustrated a comparison of different optimization algorithms (ACO, GWO, and FPA) to adjust the PID controller's settings for the optimal position and speed responses from the PMDC motor. The simulation results show the effectiveness of these algorithms under different cases of PMDC motor conditions (no load, load, and desired references for speed and position). The results illustrated the GWO gives the best response with minimum error. It can be used these proposed algorithms in speed control of the other types of DC motors. In future works, the use of on-line algorithms can improve the performance of PMDC motor.

REFERENCES

[1] Yang, Y.P., Lin, H.C., Tsai, F.C., Lu, C.T., Tu, K.H.

(2012). Design and integration of dual power wheels with rim motors for a powered wheelchair. IET Electric Power Applications, 6(7): 419-428. https://doi.org/10.1049/iet-epa.2011.0334

[2] Cheng, M., Sun, L., Buja, G., Song, L.H. (2015). Advanced electrical machines and machine-based systems for electric and hybrid vehicles. Energies, 8(9): 9541-9564. https://doi.org/10.3390/en8099541

[3] Karnavas, Y.L., Chasiotis, I.D., Amoutzidis, S.K. (2015). Design considerations and analysis of in-wheel permanent magnet synchronous motors for electric vehicles applications using FEM. In Proceedings of 17th International Symposium on Electromagnetics Fields in Mechatronics, Electrical and Electronic Engineering (ISEF), Lodz, Poland, pp. 10-12.

[4] Patil, S.S., Bhaskar, P. (2009). Design and real time implementation of integrated fuzzy logic controller for a high speed PMDC motor. International Journal of Electronic Engineering Research, 1(1): 13-25. http://www.ripublication.com/ijeer.htm.

[5] Niu, B., Zhu, Y.L., He, X.X., Zeng, X.P. (2006). Optimum design of PID controllers using only a germ of intelligence. In 2006 6th World Congress on Intelligent Control and Automation, Dalian, China, pp. 3584-3588. https://doi.org/10.1109/WCICA.2006.1713037

[6] Bansal, H.O., Sharma, R., Shreeraman, P.R. (2012). PID controller tuning techniques: A review. Journal of Control Engineering and Technology, 2(4): 168-176.

[7] Abd El Ghaffar, T.S., El-Wakeel, A.S., Eliwa, A., Mostafa, R.M. (2011). Optimal position control of permanent magnet DC motor (PMDC). In International Conference on Aerospace Sciences and Aviation Technology, Semarang, Indonesia, pp. 1-10. https://doi.org/10.21608/asat.2011.23430

[8] Gowthaman, E., Balaji, C.D. (2013). Self tuned PID based speed control of PMDC drive. In 2013 International Mutli-Conference on Automation, Computing, Communication, Control and Compressed Sensing (iMac4s), Kottayam, India, pp. 686-692. https://doi.org/10.1109/iMac4s.2013.6526496

[9] Gücin, T.N., Biberoğlu, M., Fincan, B., Gülbahçe, M.O. (2015). Tuning cascade PI(D) controllers in PMDC motor drives: A performance comparison for different types of tuning methods. In 2015 9th International Conference on Electrical and Electronics Engineering (ELECO), Bursa, Turkey, pp. 1061-1066. https://doi.org/10.1109/ELECO.2015.7394556

[10] Tuna, M., Fidan, C.B., Kocabey, S., Görgülü, S. (2015). Effective and reliable speed control of permanent magnet DC (PMDC) motor under variable loads. The Korean Institute of Electrical Engineers, 10(5): 2170-2178. https://doi.org/10.5370/JEET.2015.10.5.2170

[11] Charles, M.O., Oku, D.E., Faithpraise, F.O., Obot, E.P. (2015). Simulation and control of PMDC motor current and torque. International Journal of Advanced Scientific and Technical Research, 7(5): 367-375. http://www.rspublication.com/ijst/index.html.

[12] Sankardoss, V., Geethanjali, P. (2017). PMDC motor parameter estimation using bio-inspired optimization algorithms. IEEE Access, 5: 11244-11254. https://doi.org/10.1109/ACCESS.2017.2679743

[13] Hasan, F.A., Rashad, L.J. (2019). Fractional-order PID controller for permanent magnet DC motor based on PSO algorithm. International Journal of Power Electronics and Drive Systems, 10(4): 1724-1733. https://doi.org/10.11591/ijpeds.v10.i4.pp1724-1733

[14] Abdulhussein, K.G., Yasin, N.M., Hasan, I.J. (2021). Comparison between butterfly optimization algorithm and particle swarm optimization for tuning cascade PID control system of PMDC motor. International Journal of Power Electronics and Drive Systems, 12(2): 736-744. https://doi.org/10.11591/ijpeds.v12.i2.pp736-744

[15] Debes, R.S., Kara, T. (2022). Design and simulation of a PID neural network controller for PMDC motor speed and position control. Avrupa Bilim ve Teknoloji Dergisi, 44: 46-50. https://doi.org/10.31590/ejosat.1222247

[16] Çelik, E., Bal, G., Öztürk, N., Bekiroglu, E., Houssein, E.H., Ocak, C., Sharma, G. (2024). Improving speed control characteristics of PMDC motor drives using nonlinear PI control. Neural Computing and Applications, 36: 9113-9124. https://doi.org/10.1007/s00521-024-09568-3

[17] Sharaf, A.M., Ozkop, E., Altas, I.H. (2007). A hybrid photovoltaic PV array-battery powered EV-PMDC drive scheme. In 2007 IEEE Canada Electrical Power Conference, Montreal, Canada, pp. 37-43. https://doi.org/10.1109/EPC.2007.4520303

[18] Bae, J., Cho, K., Lee, D.H. (2020). Parallel position control scheme of permanent magnet DC motors with a low-resolution sensor. In 2020 IEEE International Conference on Industrial Technology (ICIT), Buenos Aires, Argentina, pp. 199-204. https://doi.org/10.1109/ICIT45562.2020.9067269

[19] Nekad, H.J., Shary, D.K., Alawan, M.A. (2024). Position control of linear synchronous reluctance motor using a modified camel traveling algorithm-based proportional integral controller. Mathematical Modelling of Engineering Problems, 11(6): 1585-1592. https://doi.org/10.18280/mmep.110619

[20] Shary, D.K., Nekad, H.J., Alawan, M.A. (2023). Speed control of brushless DC motors using (conventional, heuristic, and intelligent) methods-based PID controllers. Indonesian Journal of Electrical Engineering and Computer Science, 30(3): 1359-1368. https://doi.org/10.11591/ijeecs.v30.i3.pp1359-1368

[21] Dorigo, M., Birattari, M., Stutzle, T. (2006). Ant colony optimization. IEEE Computational Intelligence Magazine, 1(4): 28-39. https://doi.org/10.1109/MCI.2006.329691

[22] Martens, D., De Backer, M., Haesen, R., Vanthienen, J., Snoeck, M., Baesens, B. (2007). Classification with ant colony optimization. IEEE Transactions on Evolutionary Computation, 11(5): 651-665. https://doi.org/10.1109/TEVC.2006.890229

[23] Kouassi, B.A., Zhang, Y., Ouattara, S., Kiki, M.J.M. (2019). PID tuning of chopper fed speed control of DC motor based on ant colony optimization algorithm. In 2019 IEEE 3rd International Electrical and Energy Conference (CIEEC), Beijing, China, pp. 407-412. https://doi.org/10.1109/CIEEC47146.2019.CIEEC-2019179

[24] Yin, Z.G., Du, C., Liu, J., Sun, X.D., Zhong, Y.R. (2017). Research on autodisturbance-rejection control of induction motors based on an ant colony optimization algorithm. IEEE Transactions on Industrial Electronics, 65(4): 3077-3094. https://doi.org/10.1109/TIE.2017.2751008

[25] Oshaba, A.S., Ali, E.S., Abd Elazim, S.M. (2017). Speed

control of SRM supplied by photovoltaic system via ant colony optimization algorithm. Neural Computing and Applications, 28: 365-374. https://doi.org/10.1007/s00521-015-2068-8

[26] Mirjalili, S., Mirjalili, S.M., Lewis, A. (2014). Grey wolf optimizer. Advances in Engineering Software, 69: 46-61. https://doi.org/10.1016/j.advengsoft.2013.12.007

[27] Qais, M.H., Hasanien, H.M., Alghuwainem, S. (2018). A grey wolf optimizer for optimum parameters of multiple PI controllers of a grid-connected PMSG driven by variable speed wind turbine. IEEE Access, 6: 44120-44128. https://doi.org/10.1109/ACCESS.2018.2864303

[28] Dutta, P., Nayak, S.K. (2021). Grey wolf optimizer based PID controller for speed control of BLDC motor. Journal of Electrical Engineering & Technology, 16: 955-961. https://doi.org/10.1007/s42835-021-00660-5

[29] Sun, X.D., Hu, C.C., Lei, G., Guo, Y.G., Zhu, J.G. (2019). State feedback control for a PM hub motor based on gray wolf optimization algorithm. IEEE Transactions on Power Electronics, 35(1): 1136-1146. https://doi.org/10.1109/TPEL.2019.2923726

[30] Sun, X.D., Jin, Z.J., Cai, Y.F., Yang, Z.B., Chen, L. (2020). Grey wolf optimization algorithm based state feedback control for a bearingless permanent magnet synchronous machine. IEEE Transactions on Power Electronics, 35(12): 13631-13640. https://doi.org/10.1109/TPEL.2020.2994254

[31] Puangdownreong, D., Hlungnamtip, S., Thammarat, C., Nawikavatan, A. (2017). Application of flower pollination algorithm to parameter identification of DC motor model. In 2017 International Electrical Engineering Congress (iEECON), Pattaya, Thailand, pp. 1-4. https://doi.org/10.1109/IEECON.2017.8075889

[32] Yang, X.S., Karamanoglu, M., He, X. (2014). Flower pollination algorithm: A novel approach for multiobjective optimization. Engineering Optimization, 46(9): 1222-1237. https://doi.org/10.1080/0305215X.2013.832237

[33] Pandya, K.S., Dabhi, D.A., Joshi, S.K. (2015). Comparative study of bat & flower pollination optimization algorithms in highly stressed large power system. In 2015 Clemson University Power Systems Conference (PSC), Clemson, USA, pp. 1-5. https://doi.org/10.1109/PSC.2015.7101677

[34] Mergos, P.E., Yang, X.S. (2021). Flower pollination algorithm parameters tuning. Soft Computing, 25(22): 14429-14447. https://doi.org/10.1007/s00500-021-06230-1

NOMENCLATURE

B	Damping coefficient, Ns/rad./sec.
E	Electromagnetic force, V
i	Current, A
j	Inertia, Kg.m^2
K	Constant
L	Inductance, H
R	Resistance, Ω
T	Torque, N.m.
V	Voltage, V

Greek symbols

θ	Position, rad.
ω	Speed, rad./sec.

Subscripts

a	armature
b	back
D	derivative
e	electromanetic
I	integral
L	load
P	proportional
t	torque
v	velocity